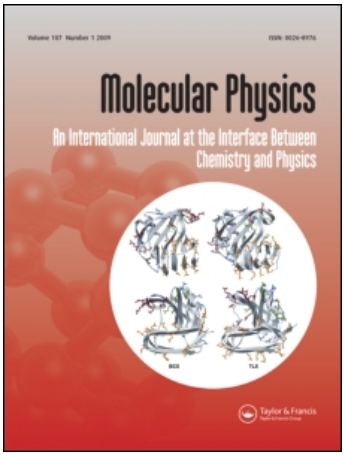

Molecular Physics
Publication details, including instructions for authors and subscription information:
http://www.informaworld.com/smpp/title~content=t713395160

Multiple hydrogen location in a vacancy region of a FCC iron-nickel-based alloy

S. Simonetti[ab]; G. Brizuela[b]; A. Juan[b]
[a] Centro de Investigaciones en Mecánica Teórica y Aplicada, Universidad Tecnológica Nacional, 8000 Bahía Blanca, Argentina [b] Departamento de Física, Universidad Nacional del Sur, 8000 Bahía Blanca, Argentina

Online publication date: 13 January 2010

To cite this Article Simonetti, S. , Brizuela, G. and Juan, A.(2010) 'Multiple hydrogen location in a vacancy region of a FCC iron-nickel-based alloy', Molecular Physics, 108: 1, 79 — 86
To link to this Article: DOI: 10.1080/00268970903512847
URL: http://dx.doi.org/10.1080/00268970903512847

Molecular Physics
Vol. 108, No. 1, 10 January 2010, 79–86

Taylor & Francis
Taylor & Francis Group

Multiple hydrogen location in a vacancy region of a FCC iron–nickel-based alloy

S. Simonetti[ab]*, G. Brizuela[b] and A. Juan[b]

[a]*Centro de Investigaciones en Mecánica Teórica y Aplicada, Universidad Tecnológica Nacional, 11 de Abril 461, 8000 Bahía Blanca, Argentina;* [b]*Departamento de Física, Universidad Nacional del Sur, Av. Alem 1253, 8000 Bahía Blanca, Argentina*

(*Received 21 June 2009; final version received 25 November 2009*)

The interaction between four-hydrogen atoms and a FCC FeNi-based alloy ideal structure having a vacancy (V) was studied using a cluster model and a semi-empirical theoretical method. The energy of the system was calculated by the atom superposition and electron delocalisation molecular orbital (ASED-MO) method. The electronic structure was studied using the concept of density of states (DOS) and crystal orbital overlap population (COOP) curves. After a sequential absorption, the hydrogen atoms are finally positioned at their energy minima configurations, near to the vacancy. The energy difference for H agglomeration was also computed. The vacancy–H_n complexes become less stable for $n>3$. The changes in the electronic structure of Fe and Ni atoms near to the vacancy were also analysed. The interactions mainly involve Fe and Ni, 4s and 4p atomic orbitals. The contribution of 3d orbitals is much less important. The Fe–Fe, Fe–Ni and Ni–Ni bonds are weakened as new Fe–H, Ni–H and H–H pairs are formed. The effect of the H atoms is limited to its first neighbours. The detrimental effect of H atoms on the metallic bonds can be related to the decohesion mechanism for H embrittlement.

Keywords: hydrogen; alloy; computer modelling and simulation; vacancy; electronic structure

1. Introduction

The electronic properties and magnetic behaviour of FeNi alloys have been of special interest since 1897 when Guillaume [1] first reported an almost zero thermal expansion over a wide temperature range in FCC crystals with Ni concentration of around 35 at.%. This behaviour was subsequently observed in various ordered and random binary alloy systems, and became known as the 'INVAR effect' [2].

The more interesting properties of the FeNi alloys are its low expansion, its electrical resistance, shape memory and soft magnetisation. The technological relevance of these alloys has been frequently related to its long-range chemical order and the similar atomic size of the atoms that explain some of their physical properties [3]. FeNi forms a solid solution in all concentrations, but the more interesting in the FCC phase starts at 28% of Ni. In this region, some useful alloys are present: Permalloy A, B and INVAR [4,5].

Vaderruten *et al*. have reported, the co-existence of BCC and FCC phases in the $22<x<40\%$ at Ni. The XRD experiments determined a lattice parameter in the BCC phase of 2.86 Å, while for the FCC phase the value is 3.59 Å. These parameters are concentration independent due to the similarity in the Fe and Ni atomic size in such a way that Fe or Ni interchange does not affect the lattice parameters [6].

On the other hand, hydrogen degradation of the structural properties of solids, referred to as embrittlement, is a fundamental problem in materials physics and metallurgy [7]. Despite intense studies, the definitive mechanism of hydrogen embrittlement in metals remains poorly understood. Four general mechanisms have been proposed: (i) formation of a hydride phase; (i) enhanced local plasticity; (iii) grain boundary weakening; and (iv) blister and bubble formation [8]. The underlying atomic processes and relative importance of the four mechanisms remain uncertain, and it is likely that a combination of these processes may contribute to embrittlement simultaneously. For these mechanisms to be operational, however, a critical local concentration of hydrogen is required, either to form a hydride phase or to initiate cracking at microvoids and grain boundaries. One of the problems in the theories of hydrogen embrittlement is the lack of a comprehensive and coherent atomistic mechanism to account for the critical hydrogen concentrations at crack tips. It is generally believed that dislocations are central to

*Corresponding author. Email: ssimonet@uns.edu.ar

ISSN 0026–8976 print/ISSN 1362–3028 online

DOI: 10.1080/00268970903512847
http://www.informaworld.com

hydrogen embrittlement phenomena, and a large body of work has been dedicated to elucidate hydrogen–dislocation interaction [8–10]. Vacancies, frequently present in the solids, have the ability to act as impurity traps and could play central role in the embrittlement process, but detailed arguments about this role or estimates of its relative importance are rather scarce.

Recent experiments on H–metal systems offer clues on the role that vacancies may play in H embrittlement. One set of experiments has established that H could induce a superabundant vacancy formation in a number of transition metals [11,12]. The estimated vacancy concentration in these systems can reach a value as high as at 23% [11]. H atoms, originally at interstitial positions in the bulk, are trapped at vacancies in multiple numbers with rather high binding energies. It was speculated that several (three to six) H atoms could be trapped by a single vacancy, with the highest number (six) corresponding to the number of octahedral sites around a vacancy in either the FCC or the BCC lattice [11,12]. However, there is a competition between monovacancy-H occupation or multiple H occupation in terms of the energy of the system and was called 'agglomeration energy' [13]. The consequence of H trapping is that the formation energy of a vacancy defect is lowered by a significant amount, an energy that has been defined as the 'H-trapping energy'. Such decrease in the vacancy formation energy could result in a drastic increase (10 times for pure BCC Fe) of equilibrium vacancy concentrations [14]. The superabundant vacancy formation provides more trapping sites for H impurities, effectively increasing the apparent H solubility in metals, several orders of magnitude. For example, it was observed experimentally that about 1000 at. ppm of H atoms can enter a metal accompanied by vacancy formation at the surface under aggressive H charging conditions, which should be contrasted with the equilibrium solubility of H in that metal [15]. The H-vacancy defects also clustered and formed platelets lying on the {111} planes, which directly lead to void formation or crack nucleation on the {111} cleavage planes [15].

There are few *ab initio* theoretical calculations in the open literature on the properties of Fe–Ni clusters. Kaspar and Salahub have used molecular-orbital calculations with the self-consistent-field Xα scatters-wave method to explain, from a molecular point of view, several of the INVAR anomalies [16]. Rao *et al.* studied the equilibrium geometries and the tendency of Fe and Ni to segregate, i.e. if Fe–Ni bonding is less favoured over Fe–Fe and Ni–Ni bonding [17]. Guenzburger and Ellis computed the electronic structure of the ordered phase of FeNi [18].

Liang and Sofronis published an interesting study of the hydrogen embrittlement in nickel-base alloys. In general, hydrogen was found to decrease both the macroscopic stress at which void initiation starts and reduce the energies expended on bulk deformation and interfacial separation [19].

In a previous work, our group studied a multiple H interaction in the vicinity of a BCC Fe bulk vacancy. Fe–Fe bonds surrounding the vacancy are weakened when hydrogen is present. This is due to the formation of new H–Fe bonds while hydrogen influences only its nearest metal atoms [13].

The extremely low solubility and high mobility of hydrogen made experimental studies very difficult. In this context, computational simulations are a suitable tool to address the problem. In this work we have used the atom superposition and electron delocalisation molecular orbital (ASED-MO) method and the YAeHMOP program to study the multiple hydrogen absorption near a Ni vacancy in an ordered FCC FeNi alloy. The effect of the impurity on the electronic structure of the solid and the Ni–H, Fe–H and H–H chemical bonding are also analyzed.

2. Computational method

The calculations were performed using the ASED-MO method [20–23]. The modification of the extended Hückel Molecular Orbital method (EHMO) was implemented with the YAeHMOP program [24]. Double zeta expansions of metal d orbitals were employed. The atomic parameters are listed in Table 1.

The ASED-MO is semi-empirical method, which makes a reasonable prediction of molecular and electronic structure. The EHMO method in its original form is not able to optimise geometries correctly as it lacks repulsive electrostatic interactions. This deficiency can be overcome by introducing a two-body electrostatic correction term [25]. The ASED theory is based on a physical model of molecular and solid electronic charge density distribution functions [23–26].

The adiabatic total energy values were computed as the difference between the electronic energy (E) of the system when the impurity atom is at finite distance within the bulk and the same energy when that atom is far away from the solid surface. There are many types of energies concerning electronic structure calculations.

The 'sequential hydrogen absorption energy' can be expressed as:

$$\Delta E_{\text{total}} = E(Fe_mNi_{m-1}H_n) - E(Fe_mNi_{m-1}H_{n-1}) - E(H) + E_{\text{repulsion}}$$

Table 1. Parameters for the ASED-MO calculations.

Atom	Orbital	Ionisation potential (eV)	Slater exponent (au^{-1})	Linear coefficient	Electronegativity (Pauling)
Fe	3d	9.00	5.35	0.5366	1.8
			1.80	**0.6678**	
	4s	**7.87**	**1.70**		
	4p	4.10	1.40		
Ni	3d	12.00	5.75	0.5683	2.0
			2.00	**0.6292**	
	4s	**9.635**	**1.80**		
	4p	5.99	1.50		
H	1s	13.6	1.00		2.1

where m is the size of the cluster and n is the number of hydrogens in the FeNi cluster containing a Ni vacancy.

The stability of the agglomeration of hydrogen in the FeNi alloy, that is the energy difference between the agglomeration of n hydrogens and n single hydrogen atoms in the vacancy, was also computed as:

$$\Delta E_{\text{Aggl,total}} = E(Fe_mNi_{m-1}H_n) - E(Fe_mNi_{m-1}) - n[E(Fe_mNi_{m-1}H_1) - E(Fe_mNi_{m-1})] + E_{\text{repulsion}}$$

where n is the number of hydrogens.

The repulsive energy was computed taking into account all atom–atom interactions.

To understand the interactions we used the concept of density of states (DOS) and crystal orbital overlap population (COOP) curves. The DOS curve is a plot of the number of orbitals per unit volume per unit energy. The COOP curve is a plot of the overlap population weighted DOS vs. energy. The integration of the COOP curve up to the Fermi level (E_f) gives the total overlap population of the bond specified and it is a measure of the bond strength.

3. The FeNi vacancy cluster model

The selected FeNi alloy structure no longer has cubic symmetry but is, in fact, tetragonal (L10). However, it was modelled as having cubic structure because the distortion is small [6,27] (see Figure 1). The FeNi phase (CuAu(I)) has a lattice parameter a = 3.592 Å [27]. We have studied the H absorption using a cluster formed by 179 metallic atoms, 90 Fe atoms and 89 + vacancy for Ni atoms. The metals were distributed in five close-packed FCC (111) planes, to represent the alloy defect and its environment. The selected geometry for each plane is an equilateral triangle having a distance between planes of 2.074 Å. The reference plane is the central one, which contains the vacancy. The cluster used in the calculations is shown in Figure 2(a).

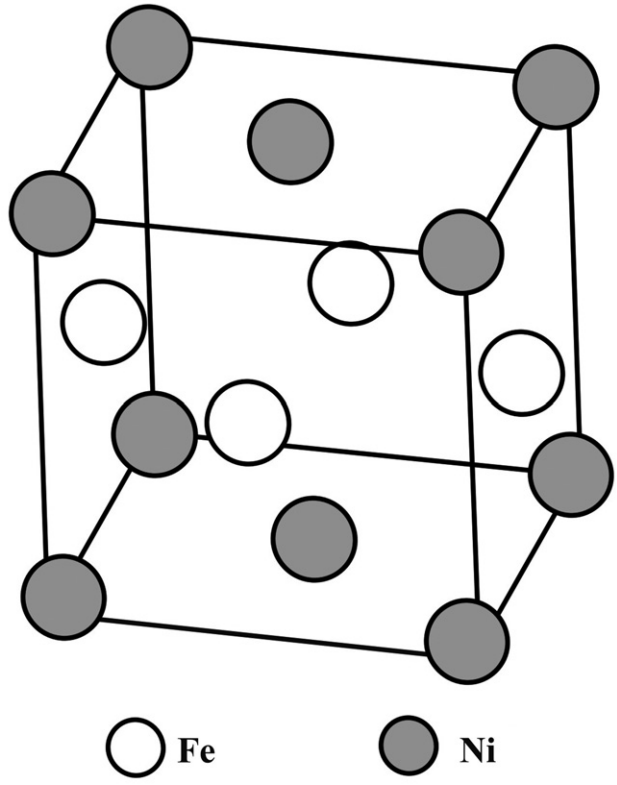

Figure 1. Conventional unit cell for the chemically ordered FeNi ideal alloy.

All of the calculations where performed at the central section of the cluster in order to avoid border effects.

The analysis of the theoretical results was performed using the energy contour plots, corresponding to the FeNi–H interaction mainly at the vacancy zone, covering all the (110) plane at steps of 0.05 Å. After determining the most stable position for the H atoms inside the cluster, the electronic structure of the FeNi–H system was computed. The Hs were sequentially absorbed.

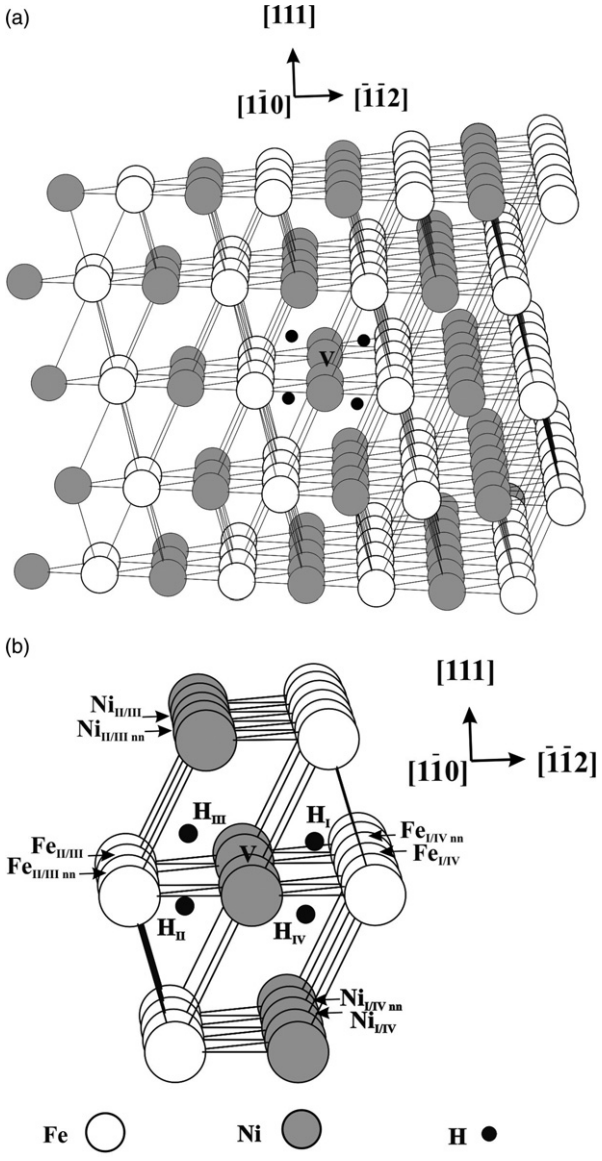

Figure 2. (a) The FeNi–H cluster containing the vacancy (V). (b) Lateral view of the vacancy region.

4. Results and discussion

Considering the sequential absorption scheme, up to four hydrogen atoms was located in the monovacancy region of the FeNi cluster. The energy associated at each formed subsystem is presented in Table 2. The sequential absorption is a favourable process, for such absorption the total energy difference is always negative. The positions of lower energy result to be those close to the vacancy (V) (see Table 2 and Figure 2(a)). The first H is eccentrically located in the vacancy at a distance of 1.322 Å from its centre and near a tetrahedral site (0.48 Å from it). It is 0.69 eV more stable than the same location in the perfect alloy and

Table 2. Sequential hydrogen absorption energy (ΔE_{Abs}), agglomeration energy (ΔE_{Agg}) and distances from H_n to the vacancy.

	Distance to the vacancy (Å)	Energy (eV)	
		ΔE_{Abs}	ΔE_{Agg}
H_I	1.322	−5.977	–
H_{II}	1.227	−6.003	−0.025
H_{III}	1.218	−5.227	0.725
H_{IV}	1.218	−5.233	1.468

the H atom is charged negatively, as was previously reported by us and others [13,28].

The minimum Fe–H distances lay between 1.623 Å and 1.689 Å of its first neighbour Fe (see Table 3). These distances are close to those computed by Juan and Hoffmann for H located near a vacancy in BCC Fe [29].

The H–vacancy distances are between 1.22 and 1.30 Å while the H–H interaction distance is close to 1.0 Å (see Tables 2 and 3). The last value is almost the same as that obtained by Simonetti *et al.* in the case of multiple H absorption in a BCC Fe vacancy [13].

Let us discuss the stability of the agglomeration of hydrogen in the FeNi alloy. The computed energy difference between the agglomeration of hydrogen and *n* single hydrogen atoms is presented in Table 2. All the VH_n complexes are energetically stable (see ΔE_{Abs}). For a number of H atoms equal to or higher than 3, the hydrogen prefers to be alone instead of agglomerating (see ΔE_{Agg} in Table 2). The VH_1 and VH_2 complexes present a little difference in energy, which cannot be considered significant for our calculation method. The agglomeration energy is only stable for VH_2 and we can conclude that VH_1 and VH_2 could be the major complexes in this vacancy containing FeNi alloy. Our model is dealing with a monovacancy; in a more realistic situation, there could be additional vacancies to act as hydrogens traps; indeed, the enhancement of vacancy formation by hydrogen trapping was suggested by Fukai *et al.* [11,12]. Our study reveals that the energy of two H atoms within one vacancy is very close to the energy of one H atom within a vacancy. This result indicates that for H, there is a possible competition between the formation of another VH_1 pair and the formation of a VH_2 triplet. Under normal conditions and even under irradiation, the vacancy concentration in the material is smaller than the H atom concentration and a large proportion of the vacancies may be associated to one or two H atoms, with strong binding energies. In a related work, Tateyama and Ohno investigated the stability and

Table 3. Atomic orbital occupations and net charges for the H_n and their neighboring Fe and Ni atoms. The major overlaps population values for these atoms are indicated.

Atom	s	p	d	Charge	Bond	Distance (Å)	OP	
H_I	1.195			−0.195	H_I–$Fe_{I/IV}$	1.623	0.165	
					H_I–$Ni_{I/IV}$	2.830	–	
H_{II}	1.191			−0.191	H_{II}–$Fe_{II/III}$	1.689	0.149	
					H_{II}–$Ni_{II/III}$	2.813	–	
H_{III}	1.131			−0.131	H_{III}–$Fe_{II/III}$	1.809	0.084	
					H_{III}–$Ni_{II/III}$	1.973	0.181	
H_{IV}	1.139			−0.139	H_{IV}–$Fe_{I/IV}$	1.809	0.083	
					H_{IV}–$Ni_{I/IV}$	1.973	0.187	
					H_I–H_{IV}	1.020	0.249	
					H_{II}–H_{III}	1.005	0.267	
							H	Free of H
$Fe_{I/IV}$	0.511	0.055	4.928	2.506	$Fe_{I/IV}$–$Fe_{I/IV\,nn}$	2.540	0.096	0.239
$Fe_{I/IV\,nn}$	0.510	0.051	4.913	2.526				
$Fe_{II/III}$	0.501	0.067	4.842	2.590	$Fe_{II/III}$–$Fe_{II/III\,nn}$	2.540	0.108	0.248
$Fe_{II/III\,nn}$	0.502	0.053	4.950	2.495				
$Ni_{I/IV}$	0.827	0.954	9.433	−1.213	$Ni_{I/IV}$–$Ni_{I/IV\,nn}$	2.540	0.264	0.329
$Ni_{I/IV\,nn}$	0.822	0.949	9.442	−1.214				
$Ni_{II/III}$	0.823	0.951	9.433	−1.207	$Ni_{II/III}$–$Ni_{II/III\,nn}$	2.540	0.266	0.328
$Ni_{II/III\,nn}$	0.829	0.941	9.529	−1.209				
					$Fe_{I/IV}$–$Ni_{I/IV}$	2.540	0.148	0.222
					$Fe_{II/III}$–$Ni_{II/III}$	2.540	0.143	0.218

Notes: $Fe_{I/IV}$: Fe atom first neighbour to H_I and H_{IV}; $Fe_{I/IV\,nn}$: Fe atom first neighbour to $Fe_{I/IV}$.
$Fe_{II/III}$: Fe atom first neighbour to H_{II} and H_{III}; $Fe_{II/III\,nn}$: Fe atom first neighbour to $Fe_{II/III}$.
$Ni_{I/IV}$: Ni atom first neighbour to H_I and H_{IV}; $Ni_{I/IV\,nn}$: Ni atom first neighbour to $Ni_{I/IV}$.
$Ni_{II/III}$: Ni atom first neighbour to H_{II} and H_{III}; $Ni_{II/III\,nn}$: Ni atom first neighbour to $Ni_{II/III}$.

binding properties of hydrogen–vacancy (VH_n) complexes in α-Fe. The authors demonstrated that VH_2 is the major complex in α-Fe [14].

Figure 3 shows the energy contour lines corresponding to the agglomeration energy for the VH_4 complex. We can see aligned H atoms along $\langle -1-1\ 2\rangle$ direction in the (111) plane. Tateyama and Ohno have reported that VH_2 complexes are likely to favour line clusters along the $\langle 111\rangle$ direction and also tabular one along $\{110\}$ or $\{100\}$ planes [14].

Regarding the electronic structrure, Figure 4 shows an interaction diagram. In the middle, Figure 4(b) shows the total DOS curve for the isolated FeNi system. Comparing, the total DOS curve for the FeNi–H system (Figure 4(a)) we can see two small peaks appearing below the d metal band at about −17 eV and −18 eV that corresponds to H-based states stabilised after absorption. The small contribution of Hs to the total DOS is a consequence of their low concentration. Figure 4(c) shows the projected DOS for all the H atoms. The partial electron density of these new states indicates FeNi–H 1s hybridisation. This hybridisation is responsible for the large H trapping energies for VH_2 (and VH_1) formation through the termination of broken Fe–Ni bonds. The new state has a bonding character mainly consisting of H 1s orbital and is doubly occupied by electrons. This indicates electron transfer to the region around the H atoms from the neighbour Fe. The resulting negatively charged H atoms may repel each other and the repulsive interaction seems to become more dominant with increase in the number of trapped hydrogen atoms. This can explain the abrupt decrease of H trapping energies for VH_n ($n \geq 3$).

Considering the chemical bonding, the metal–metal cohesion is dramatically changed when hydrogens are present. The OP between the metallic atoms nearest neighbour to the hydrogens decreases (see Table 3 – atom numbering indicated as in Figure 2(b)). A decrease in the OP is generally interpreted as a measure of metal-metal bond weakening. The changes in the OP between metal-metal bonds, before and after H location are shown in Figure 5. The Fe–Fe bond is the most affected, its strength decreases by about 60% while the Fe–Ni and Ni–Ni OPs decrease by about 33% and 20%, simultaneously. Fe–H and Ni–H bonds are formed and their bonding is achieved at the expense of the nearest neighbour's metal atoms.

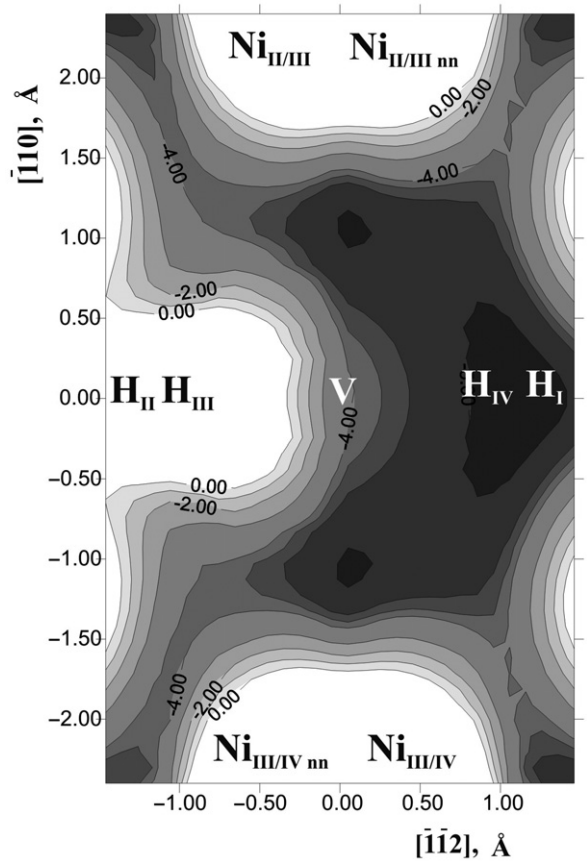

Figure 3. Contour energy plots corresponding to the energy (eV) for the FeNi–H system near the vacancy region.

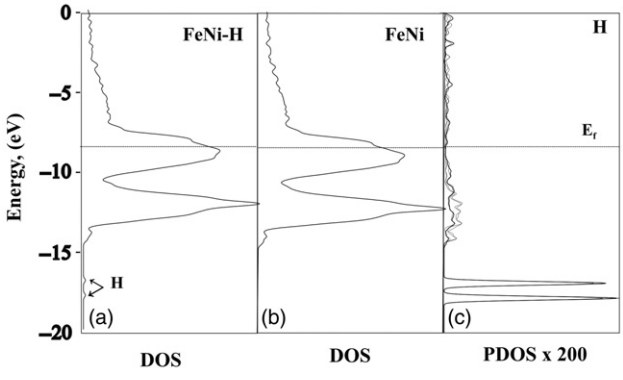

Figure 4. (a) Total DOS for the FeNi–H cluster; (b) total DOS for the clean FeNi cluster; and (c) projected DOS for the H atoms.

Our results support one of the embrittlement mechanisms: the decohesion of the metallic bond. The Fe–H and Ni–H COOP curves corresponding to the major interactions are plotted in Figure 6, as we can see, all

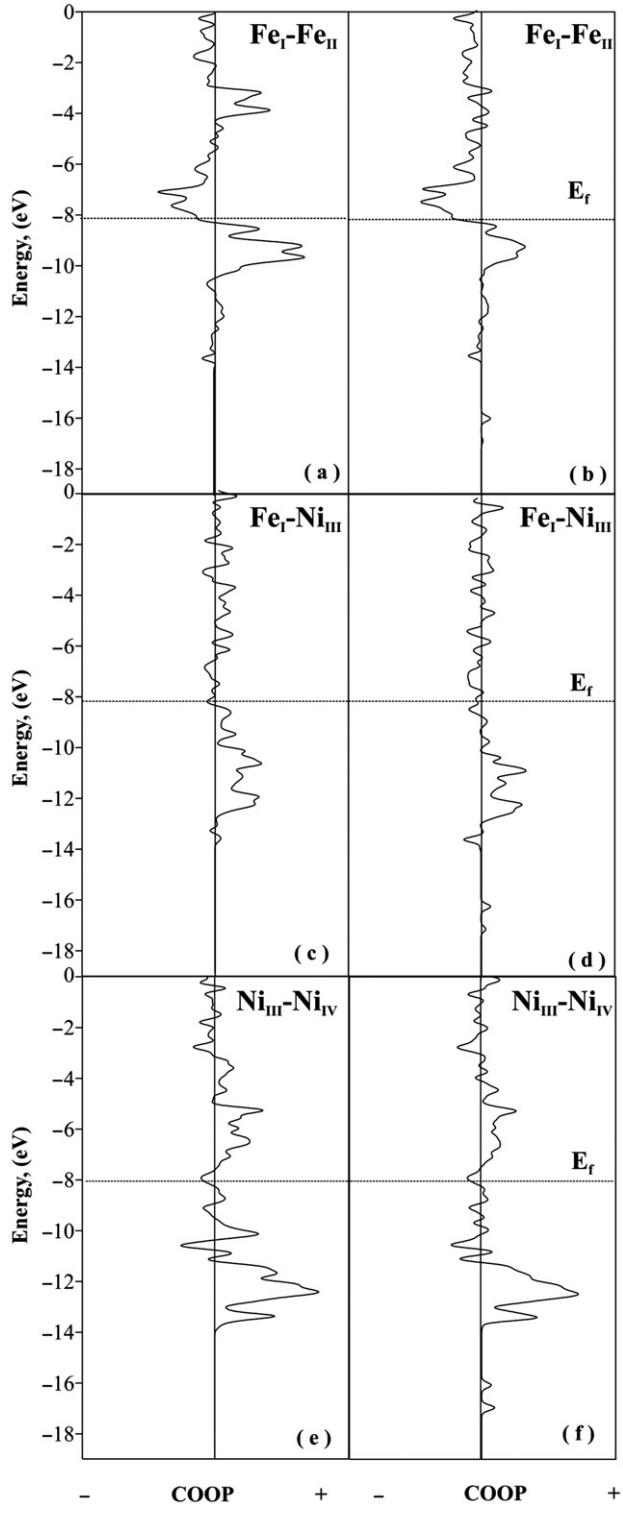

Figure 5. COOP curves for Fe_I–Fe_{III} (a) before and (b) after H adsorption. COOP curves for Fe_I–Ni_{III} (c) before and (d) after H adsorption. COOP curves for Ni_{III}–Ni_{IV} (e) before and (f) after H adsorption.

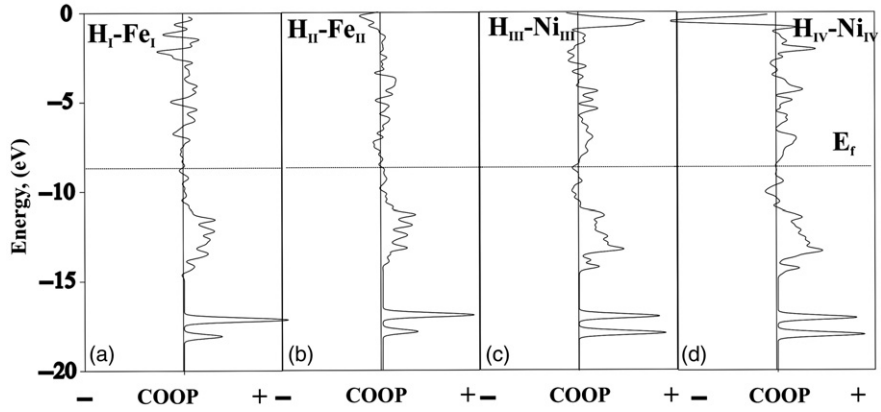

Figure 6. COOP curves for (a) and (b) H–Fe interactions, (c) and (d) H–Ni interactions near the Ni vacancy.

interactions are bonding. From Table 3, we can see that Fe–H interaction mainly involves Fe 4s and Fe 4p atomic orbitals, the contribution of Fe 3d orbitals is much less important. The contribution of Fe 4s and Fe 4p populations decreases by about 15% and 40%, respectively, with respect to the cluster without H impurities. The Fe 3d population decreases to about 7% when the hydrogens are present. On the other hand, the Ni–H interaction involves Ni 4s and Ni 4p atomic orbitals but the populations decrease by only 5% and 4%, respectively. The contribution of Ni 3d orbitals is less than 1%. The Ni–H strongest interaction has an OP value of 0.187 at 1.973 Å, while the Fe–H has an OP value of 0.165 at 1.623 Å. Atomic orbital occupations and net charges for the H atoms and their neighbouring Fe and Ni atoms are also summarised in Table 3.

When the phenomenon of multiple occupations is addressed, a question emerges: is there any chemical bond between the hydrogens? We have detected some H–H association in the cluster. The COOP curves corresponding to the more important H–H interactions are shown in Figure 7. This curves present bonding and antibonding states below the E_f. Integration up to the Fermi level gives total OP for the H–H bonding in the cluster at a distance of about 1.0 Å, with an OP value of 0.249–0.267. The strength of the H–H association might be compared with the H_2 molecule, in vacuum. Under the same ASED-MO approximations, the OP at the H_2 equilibrium distance of 0.78 Å is 0.845 while at 1.0 Å it is reduced to 0.762. At the same distance in the alloy matrix near the vacancy, the H–H pair has an OP of 0.245, which is consistent with H–metal competitions for bonding.

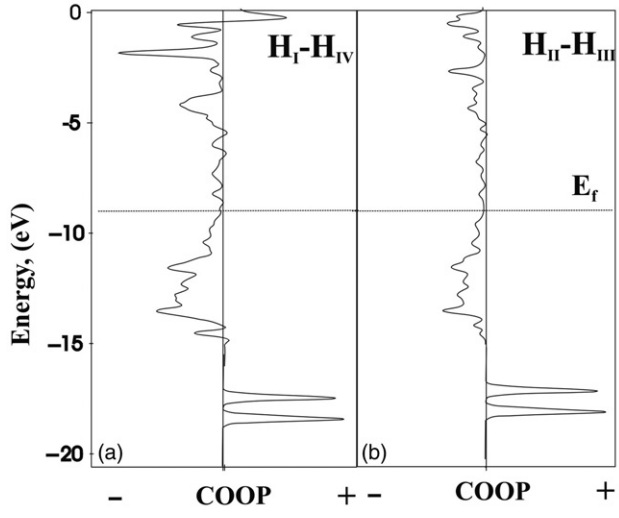

Figure 7. COOP curves for (a) H_I–H_{IV} and (b) H_{II}–H_{III} interactions near the Ni vacancy.

5. Conclusions

We studied the interaction between four hydrogen atoms on a FCC FeNi alloy with a Ni vacancy (V). H locates eccentrically to the centre of the vacancy and becomes negatively charged.

The stability of agglomeration of hydrogen reveals that VH_1 and VH_2 are the major complexes in the alloy. For more than two H atoms, agglomeration is an unfavourable process.

The presence of Hs decreases the metal–metal OP, which could be considered as a measure of the bond strength. At the same time, Fe–H and Ni–H bonds are formed at the expense of their metal–metal bonds. The interaction mainly involves metal 4s and 4p, and

H 1s orbitals. The contribution of 3d orbitals is much less important.

The H–H pair also interacts with an OP of 0.245, however, this value is only 33% of that corresponding to a similar pair in vacuum, showing the more important H–metal interaction. The detrimental effect of H on the metallic bonds and the H–H association could be related to the decohesion mechanism for hydrogen embrittlement.

Acknowledgements

Our work was supported by PIP 0103 (CONICET), PICT 560 and 1186 (ANPCyT), Departamento de Física-Universidad Nacional del Sur and Departamento de Ingeniería Mecánica-Universidad Tecnológica Nacional. The authors are members of CONICET-Argentina.

References

[1] C.E. Guillaume, C. R. Acad. Sci **125**, 235 (1897).
[2] E.F. Wassermann, in *Ferromagnetic Materials*, edited by K.H. Buchow and E.P. Wohlfarth (Elsevier, Amsterdam, 1990), Vol. 5, Chap. 3, pp. 237–322.
[3] G.E. Ice, G.S. Painter, L. Shaffer, and C.J. Sparks, NanoStruct. Mater. **7**, 147 (1996).
[4] K.B. Reuter, D.B. Williams, and J.I. Goldstein, Metall. Trans. A **20**, 71 (1988).
[5] D.G. Rancourt and R.B. Scorzelli, J. Magn. Magn. Mater. **150**, 30 (1995).
[6] J.F. Valderruten, G.A. Peréz Alcázar, and J.M. Greneche, Revista Colombiana de Física. **38**, 97 (2006).
[7] R.A. Oriani, Ann. Rev. Mater. Sci. **8**, 327 (1978).
[8] S.M. Myers, M.I. Baskes, H.K. Birnbaum, J.W. Corbett, G.G. De Leo, S.K. Estreicher, E.E. Haller, P. Jena, N.M. Johnson, R. Kirchheim, S.J. Pearton, and M.J. Stavola, Rev. Mod. Phys. **64**, 559 (1992).
[9] H.K. Birnbaum, in *Hydrogen Embrittlement and Stress Corrosion Cracking*, edited by R. Gibala and R.F. Hehemann (American Society for Metals, Ohio, 1984).
[10] S. Simonetti, M. Pronsato, G. Brizuela, and A. Juan, Appl. Surf. Sci. **217**, 56 (2003).
[11] Y. Fukai, Phys. Ser. T **Tl03**, 11 (2003).
[12] Y. Fukai and N. Okuma, Phys. Rev. Lett. **73**, 1640 (1994).
[13] S. Simonetti, C. Pistonesi, G. Brizuela, and A. Juan, J. Phys. Chem. Sol. **66**, 1240 (2005).
[14] Y. Tateyama and T. Ohno, Phys. Rev. B **67**, 174105 (2003).
[15] H.K. Birnbaum, C. Buckley, F. Zeides, E. Sirois, P. Rozenak, S. Spooner, and J.S. Lin, J. Alloys Compd. **253**–**254**, 260 (1997).
[16] J. Kaspar and D. Slahub, Phys. Rev. Lett. **47**, 54 (1981).
[17] B.K. Rao, S. Ramos de Debiaggi, and P. Jena, Phys. Rev. B **64**, 024418 (2001).
[18] D. Guenzburger and D.E. Ellis, Phys. Rev. B **36**, 6971 (1987).
[19] Y. Liang and P. Sofronis, Modelling Simul. Mater. Sci. Eng. **11**, 523 (2003).
[20] R. Hoffmann and W.N. Lipscom, J. Chem. Phys. **36**, 2179 (1962).
[21] R. Hoffmann, J. Chem. Phys. **39**, 1397 (1963).
[22] M.H. Whangbo and R. Hoffmann, J. Am. Chem. Soc. **100**, 6093 (1978).
[23] A. Anderson, J. Chem. Phys. **62**, 1187 (1975).
[24] G. Landrum and W. Glassey, *Yet Another Extended Hückel Molecular Orbital Package (YAeHMOP)* (Cornell University, Ithaca, NY, 2004).
[25] A. Anderson and R. Hoffmann, J. Chem. Phys. **60**, 4271 (1974).
[26] A. Anderson, J. Electroanal. Chem. Interfacial Electrochem. **280** (1), 37 (1990).
[27] M.-Z. Dang and D.G. Rancourt, Phys. Rev. B **53**, 2291 (1996).
[28] P. Nordlander, J.K. Nørskov, and F. Besenbacher, J. Phys. F, Met. Phys. **16**, 1161 (1986).
[29] A. Juan and R. Hoffmann, Surf. Sci. **421**, 1 (1999).